Mathematical simulation on the oil slick spreading and dispersion in nonuniform flow fields

[*]Q. Peishi; S. Zhiguo; L. Yunzhi

State Key Laboratory of Urban Water Resource and Environment, Harbin Institute of Technology, Harbin, 150090, China

ABSTRACT: The viscous fluid boundary layer equations were adopted to characterize the velocity distribution across the vertical section of the oil slick on moving water. The velocity profile was found to be the combination of linear and parabolic distribution. A numerical model including spreading and dispersion was developed to describe the oil slick's early movement in the open and ice-covered water. The flume test was conducted to determine the dispersion coefficients (K_x) and the effects of velocity and wave height on the slick's dispersion were also investigated. In the open water, K_x increased from 4.34 cm²/s to 20.08 cm²/s as the velocity changed from 3 cm/s to 12 cm/s. A coefficient β that characterized K_x fluctuated at 1.5 when wave heights were between 20 mm and 70 mm. Under ice, the slick didn't move until the velocity exceeded 6 cm/s and K_x increased from 2.69 cm²/s to 5.64 cm²/s as the velocity changed from 6 cm/s to 12 cm/s. β remained 0.4 when wave heights were between 20 mm and 60 mm. The model performed very well in predicting the slick's position and length during the gravitation-inertia phase for the two situations when relevant dispersion coefficients were input.

Keywords: *Dispersion coefficient; Flume test; Ice sheet; Oil spill*

INTRODUCTION

Accidental oil spills often cause serious impact on the environment. With the increase of oil extractions and navigation activities in rivers, riverine oil spills occur more often than before, which have been receiving particular attention by scientists and governments (Yapa and Chen, 1994; Guo *et al.*, 2008; Alihosseini *et al.,* 2010; Nagheeby and Kolahdoozan, 2010). When liquid oil is spilled, it spreads to form an oil slick on the water surface whose movement is governed by the following processes: (1) the mechanical spreading due to the balance between gravitational, viscous forces and surface-tension; (2) the drifting and advection due to the current and wind; and (3) the horizontal dispersion due to the non-uniform distribution of velocities and waves (Shen and Yapa, 1988; Wang *et al.*, 2005; Husseien *et al.,* 2009). Furthermore, the oil spreading in ice-covered rivers is much more complicated due to the interference from the ice sheet, and it is more difficult to determine the location and area of the slick under ice (Izumiyama and Konno, 2002; Fingas and Hollebone, 2003).

✉ *Corresponding Author Email: qipeishi@163.com*
   Tel.: 1390 4639 918; Fax: +86451 8232 3844

Therefore, considering the particularity of riverine and under-ice oil spills, it is essential to establish models to predict the oil spreading in the one-dimensional non-uniform flow field especially covered by ice (Tuzkaya *et al.,* 2009).

Some work has been directed towards developing models to predict the trajectory and fate of spilling oil in rivers. Fay's empirical formulae are considered as the state-of-the-art in oil slick models and are still used up to now (Guo and Wang, 2009) and their later derivatives enlarged the slick's spreading dimension along the moving direction by taking the wind and current into consideration (Zhao *et al.*, 1987; Reed *et al.*, 1999; Abbaspour and Shojaee, 2009). Advection-diffusion equations have been adopted based on the mass conservation law to compute the concentration of compounds both in the slick phase and in the aqueous phase with the solutions being obtained by Eulerian methods (EMs) and Lagrangian methods (LMs) (Hibbs *et al.*, 1999; Gong *et al.,* 2009). The random walk particle tracking (RWPT) are applied to describe the oil droplet's movement within the water column. In this method, each particle represents a fraction of the

total oil and the two-dimensional movements are simulated by taking into account the effects of the physicochemical processes on the fate of the particles (Brovchenko *et al.*, 2002; Elliot, 2004; Wu and He, 2010). Also, some models which developed from these methods are used to simulate the oil spreading under ice. Yapa and Chowdhury (1991) adopted RWPT and the Hoult's models (1969) to predict the oil drifting and spreading under ice, respectively. Yu *et al.* (1999) and Wang *et al.* (2003) reported a series of formulae to describe the oil spreading under ice with different ice-coverage rates.

The main problems of these models are as follows: Fay's formulae are mainly for the simulation of oil spreading on the clam water without too much consideration about the effects of turbulent current and wave on the slick (Liu and Sun, 2009; Guo and Wang, 2009); the advection-diffusion equations are established on the assumption that the spilled product is completely soluble or partly dissolved into the water, which is not reasonable for the early stage after an oil spill happened and the RWPT concentrates mainly on the diffusion and drifting processes. It usually underestimates the early spreading area. This can produce great deviation for instantaneous large-scale oil spills because the gravitation-inertia phase usually lasts for hours in that case (Liu and Sun, 2009).

Therefore, it seems more promising to ameliorate the Fay's model for the slick's early movement by taking into consideration the effects of flow velocity and wave. Due to the river channel's long-narrow terrain and high flow velocity, the slick will travel for a long distance along the river within 2 days. And the slick could hardly be broke up and spread to the water body vertically during such a short time (Hibbs *et al.*, 1999; Rajakumar *et al.,* 2011). Therefore, it is reasonable to adopt one-dimensional model to predict the slick's position and contaminative area. The main objective of the present work was to establish a model to account for the early oil spreading in the open water and ice-covered water with high velocities. Both the spreading and horizontal dispersion were considered. The dispersion coefficients were determined and effects of the wave on the dispersion were also investigated via the flume test conducted in the hydraulics laboratory of Harbin Institute of Technology during winter in 2008. The model mainly concentrated on the oil slick's elongating scope and the positions of the leading and tailing edges during the gravitation-inertia phase. The evaporation was neglected here and was studied in our other paper (Qi *et al.*, 2010).

Theoretical model of oil slick movement

The viscous fluid boundary layer equations are adopted to describe the velocity distribution within the oil slick (Liu and Shu, 1991). Some premises are made: the slick is presumed to be one continuous layer floating on the water surface without any breakup. The water is moving at the velocity of U_0 and the boundary layer thickness of the aqueous phase is 0. By neglecting physical and chemical changes, such as evaporation and water uptake and assuming the density and viscosity are constant, the only change that the oil can undergo is the movement from one place to another.

Kinematic analysis of oil slick on the moving water

As shown in Fig. 1, the reference frame is established and moving along with the slick center. The viscous fluid boundary layer equations are as follows:

Continuity equation:

$$\frac{\partial u}{\partial x} + \frac{\partial v}{\partial y} = 0 \qquad (1)$$

Navier-Stokes equations:
x direction:

$$u\frac{\partial u}{\partial x} + v\frac{\partial u}{\partial y} = -\frac{1}{\rho}\frac{dp}{dx} + \upsilon(\frac{\partial^2 u}{\partial x^2} + \frac{\partial^2 u}{\partial y^2}) \qquad (2)$$

y direction:

$$u\frac{\partial v}{\partial x} + v\frac{\partial v}{\partial y} = -\frac{1}{\rho}\frac{dp}{dy} + \upsilon(\frac{\partial^2 v}{\partial x^2} + \frac{\partial^2 v}{\partial y^2}) \qquad (3)$$

Considering the slick is moving along the x direction, v = 0, and Eq. 1 becomes:

$$\frac{\partial u}{\partial x} = 0 \qquad (4)$$

It is realized that u is the function of y, which can be expressed as:
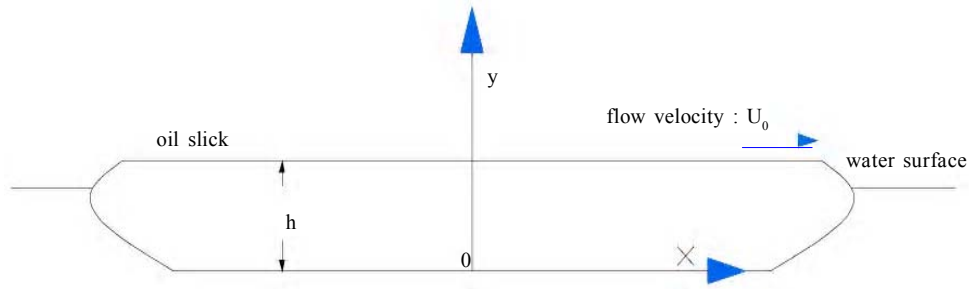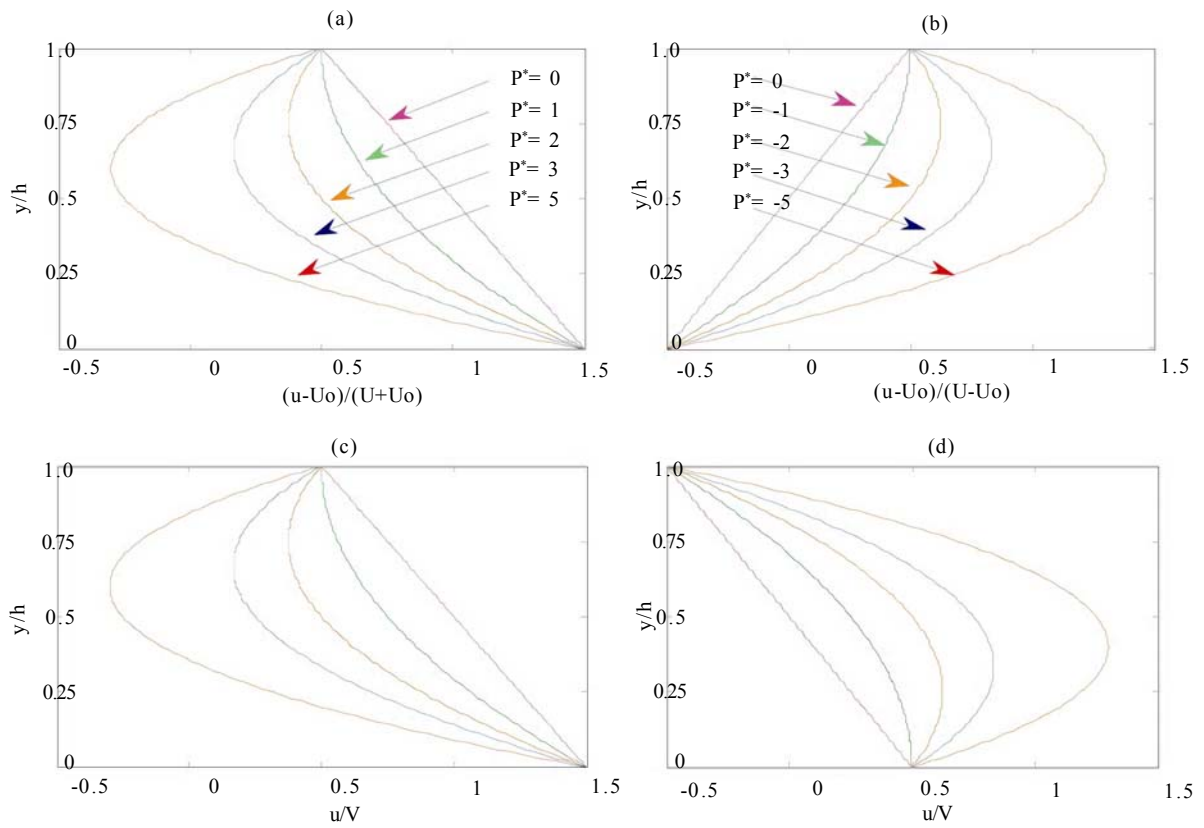
$$u = u(y) \qquad (5)$$

Fig.1: Sketch map of the oil slick spreading on the moving water

(a). for the slick behind the spilling center (b). for the slick in front of the spilling center
(c). for the slick behind the spilling center under ice (d). for the slick in front of the spilling center under ice

Fig.2: Dimensionless velocity distributions within the oil slick

And the N-S equations can be simplified as:

$$-\frac{dp}{dx} + \mu\frac{\partial^2 u}{\partial y^2} = 0 \qquad (6)$$

$$\frac{dp}{dy} = 0 \qquad (7)$$

According to Eq. 7, it is known that p is the function of x. Considering $u = u(y)$, dp/dx in (6) is a constant. Then, N-S equations are changed into the following ordinary differential equation:

$$\mu\frac{\partial^2 u}{\partial y^2} - \frac{dp}{dx} = 0 \qquad (8)$$

The top layer of the oil slick is assumed to be moving at the velocity of U, and the bottom layer was moving at U_0 ($U_0 < U$), the same velocity as water, and the boundary conditions are:
u=U, y=h;
u= U_0 ÿ y=0;
The following equation is obtained by integrating Eq. 8:

$$u = U_o + (U - U_o)\frac{y}{h} - \frac{h^2}{2\mu}\frac{dp}{dx}\frac{y}{h}(1 - \frac{y}{h}) \qquad (9)$$

The first two terms on the right are produced by the daggling effect of water and the velocity profile is the linear distribution across the vertical section within the slick. The third term is produced by the pressure gradient due to the asymmetry in the slick's thickness and the velocity profile is the parabolic distribution (Liu and Shu, 1991; Zhang and Dong, 1998), both of which related to the oil viscosity; the higher the oil viscosity is, the larger the difference in the velocity between the top and bottom layers is. Therefore, the slope of the linear distribution and the concave curvature of the parabolic distribution are both greater (Zhang and Dong, 1998). Eq. 9 is handled dimensionlessly as follows:

$$u* = y* - p* y*(1 - y*) \qquad (10)$$

Where: $u* = \frac{u - U_o}{U - U_o}$, $y* = \frac{y}{h}$,

$$p* = \frac{h^2}{2\mu(U - U_o)}\frac{dp}{dx}$$

are called dimensionless speed, dimensionless distance and dimensionless pressure gradient, respectively. With p* as input parameters, the velocity profile across the vertical section within the slick was plotted in Fig. 2. For the first half part before the slick center, dp/dx < 0, the slick and water were moving in the same direction. The slick spreading was down-pressure flow as shown in Fig. 2b. It was concluded that the spreading speed decreased gradually with time and the pressure gradient decreased correspondingly. Also, it was find that the pressure gradient would be smaller for the surrounding part which stayed farther away from the slick center. While the slick was getting thinner, the difference in the velocity between top and bottom layers was smaller, and U was getting close to U_0. For the other part behind the slick center, dp/dx> 0, the slick and water were moving in the opposite directions. The slick spreading was called against-pressure flow as shown in Fig. 2a. The bottom layer of the slick was moving forwards with water while the top layer was moving backwards, which was defined as circumfluence (Zhang and Dong, 1998; Guo, 2008). As the slick was spreading, the absolute value of dp/dx decreased gradually. Due to the daggling effect of water, the circumfluence speed decreased to 0 and began to flow forwards with water. After then, the slick was getting further thinner and the pressure gradient disappeared, and U was getting close to U_0 finally.

For the slick under ice, the velocity at the bottom layer of the slick is V (V<U_o) while the velocity at the top layer is related to the roughness of the ice sheet. For the smooth ice sheet, u|$_{y=h}$=U>0, Eqs. 9 and 10 are used to describe the velocity distribution within the slick. And for the rough ice sheet:

u|$_{y=h}$=0, the boundary conditions are:
u=0, y=h; u= V, y=0;

Eq. 8 is integrated and the following equation is obtained:

$$u = V\frac{y}{h} - \frac{h^2}{2\mu}\frac{dp}{dx}\frac{y}{h}(1 - \frac{y}{h}) \qquad (11)$$

Handling Eq. 11 dimensionlessly as follows:

$$u* = y* - p*y*(1-y*) \qquad (12)$$

Where : $u* = \dfrac{u}{V}, \qquad y* = \dfrac{y}{h},$

$$p* = \dfrac{h^2}{2\mu V}\dfrac{dp}{dx}$$

In Fig. 2, the velocity distribution across the vertical section within the slick under the ice sheet was also plotted with p* as input parameters. For the first half part before the slick center, dp/dx < 0, the slick and water were moving in the same direction. The slick spreading was down-pressure flow and was shown in Fig. 2d. For the other part behind the slick center, dp/dx > 0, the slick and water were moving in the opposite directions. The slick spreading was against-pressure flow and was shown in Fig. 2c.

Spilled oil model

As it is difficult to determine the value of dp/dx, it is almost impossible to obtain the analytical solutions by solving the N-S equations mentioned above. The following equations were adopted to predict the oil spreading in one-dimensional flow fields.

$$L = d_f + d_x \qquad (13)$$

Where df is the spreading dimension and will be calculated according to Fay's model, dx is the dispersion dimension of the oil slick along the longitudinal direction and will be studied via the flume test. Therefore, the oil extending is the synthetical effect of the spreading and dispersion (Zhao *et al.,* 1987).

Oil spreading in open water

Spreading is the horizontal expansion of the oil slick, which is driven by the gravity with the inertial force being the main retarding force in the early stage (Guo and Wang, 2009). The classical one-dimensional spreading models developed by Fay are used here focusing on the gravitation-inertial phase:

$$d_f = 1.5(\Delta g W t^2)^{1/3} \qquad (14)$$

where $\Delta = 1 - (\rho_o / \rho_w)$, ρ_o and ρ_w are densities of oil and water, respectively, W is the volume of the oil per unit length, g is the gravity acceleration, t is the spreading time. The duration of this phase can be calculated as:

$$t_{12} = [(\Delta g)^2 \nu_w^{\ 3}]^{-1/7} W^{4/7} \qquad (15)$$

where ν_w is the kinematic viscosity of water.

Oil spreading under ice

It is widely recognized that the driven force under ice is the buoyancy force, which is equivalent to the gravity in open water. The buoyancy-inertia phase lasts for only a short period of time while the buoyancy-viscous phase appears to last for a much longer time. It is also observed that the interfacial tension-viscous phase does not exist under ice (Izumiyama and Konno, 2002; GjØsteen, 2004). Shen and Yapa (1988) proposed some formulae to simulate the oil spreading under the ice sheet:
Buoyancy-inertia phase:

$$R = 0.751[(\dfrac{\rho_w}{\rho_o} - 1)gV]^{1/4} t^{1/2} \qquad (16)$$

And the duration of this phase is:

$$t = (\dfrac{k}{0.751})^{8/3}[\dfrac{V\rho_o^{\ 2}}{\mu_o(\rho_w - \rho_o)g}]^{1/3} \qquad (17)$$

where R is the radius of the oil slick under ice, k is a constant (k = 0.508), μ_o is the kinematic viscosity of oil. Because little is known about the one-dimensional spreading under ice, Eq. 16 has to be corrected by flume test results before being adopted.

Dispersion of the oil slick

Considering the shear force of the turbulent current acting on the slick's bottom surface, the slick can be elongated along the flow direction, which is defined as the dispersion. The dispersion model was written as:

$$\dfrac{\partial h}{\partial t} = K_x \dfrac{\partial^2 h}{\partial x^2} + K_y \dfrac{\partial^2 h}{\partial y^2} - kh \qquad (18)$$

where h is the slick's thickness, k is the attenuation coefficient and is neglected here owing to the above assumptions, x and y are coordinates along the drifting

direction and perpendicular to the drifting direction, respectively. K_x and K_y, in the dimension of cm^2/s are the dispersion coefficients along direction x and y. Assuming they are not variable with time and space, the analytical solution of Eq. 18 is:

$$h = \frac{V_o}{\sqrt{4\pi K_x K_y t}} \exp[-\frac{x^2}{4K_x t} - \frac{y^2}{4K_y t}] \qquad (19)$$

where V_o is the initial volume of the oil. K_y can be neglected in the one-dimension flow field, and Eq. 19 becomes:

$$h = \frac{V_o}{\sqrt{4\pi K_x t}} \exp(-\frac{x^2}{4K_x t}) \qquad (20)$$

And the slick's dispersion dimension along the longitudinal direction can be calculated as:

$$d_x = \omega\sigma_x = \omega\sqrt{2K_x t} \qquad (21)$$

Where σ_x is the standard derivation of the slick's thickness along the direction x, ω and K_x ($\omega=1$ in this condition) are determined according to the experimental results instead of adopting the experiential formulae reported by Zhao *et al.,* (1987) because d_x here is used to describe the slick's dispersion in the one-dimensional flow field but not at sea. Flume experiments by Sayre and Chang (1969) indicated that K_x for floating dispersants was approximately the same as that for dissolved dispersants and could still be expressed in the form of βDu^* (Shen and Yapa, 1988). β is an empirical coefficient and is determined according to the experimental results. D is the virtual depth of the water. u^* is the shear velocity and can be calculated according to the following equation:

$$\frac{v}{u} = 1 + \frac{u^*}{\kappa u} \qquad (22)$$

where v is the water surface velocity, u is the average velocity, κ (= 0.4) is the Karman constant. The ratio v/u takes the value of 1.1(Shen and Yapa, 1988).

Oil drifting in open water

The main purpose in calculating the slick drifting is to predict the contaminative scope and location with time and take corresponding emergent action. Almost all the oil slick drifting models are based on the combined effects of the surface current and wind (Hibbs *et al.*, 1999; Boufadel *et al.*, 2007):

$$u_o = \alpha_{vel}u + \alpha_{wind}u_{wind} \qquad (23)$$

where u_o is the drifting speed of the slick's centroid, u_{wind} is the wind speed at 10 m above the water surface, α_{vel} is the velocity profile correction factor (α_{vel}=1.1), and α_{wind} is the wind drift coefficient (α_{wind}=0.035). The wind drift term is dropped here, and the velocities of the leading and trailing edges of the slick are:

$$u_{leading} = 1.1u + \frac{dL}{dt} \qquad (24)$$

$$u_{trailing} = 1.1u - \frac{dL}{dt} \qquad (25)$$

where dl/dt is the spreading rate of the slick. The positions of the leading and tailing edges can be predicted according to the following equations:

$$X_l = u_{leading}t = 1.1ut + 0.5L \qquad (26)$$

$$X_t = u_{trailing}t = 1.1ut - 0.5L \qquad (27)$$

where X_l and X_t are the coordinates of the slick's leading and tailing edges with the pouring point being the origin.

Oil drifting under ice

The slick drifting under ice is related to the ice sheet's roughness, velocity and characteristics of oil. Generally, the oil will be congregated under the rough ice sheet. Under the smooth ice sheet, the slick will drift with water when the velocity exceeds a certain value (Yapa and Chowdhury, 1991). In this study, the ice sheet is smooth and the roughness height is smaller than the equilibrium slick thickness δ_{eq}. Yapa and Shen (1994)

suggested the threshold velocity, at which the oil slick began to drift, was calculated as:

$$u_{th} = \frac{305.79}{88.68 - \mu_o} \qquad (28)$$

The equilibrium thickness (δ_{eq}) can be determined by the following equation:

$$\delta_{eq} = 1.67 - 8.5(\rho_w - \rho_o) \qquad (29)$$

If the depth-averaged velocity is greater than the threshold velocity, the slick will drift downstream with the current and the relation between the velocity and the slick's drifting speed is given as:

$$(1 - \frac{u_o}{u})^2 = \frac{K}{0.115 F_\delta^2 + 1.105} \qquad (30)$$

where u_o is the slick's drifting speed, K is the friction amplification factor, and is assumed to vary linearly between 1.0 for a smooth cover and 2.6 for an ice cover with Manning's roughness coefficient $n_i = 0.055$, F_δ is a dimensionless number which can be calculated as:

$$F_\delta = \frac{u}{\sqrt{\Delta g \delta_{eq}}} \qquad (31)$$

MATERIALS AND METHODS

The simulation test was conducted in the cycled vitreous flume in the hydraulics laboratory of Harbin Institute of Technology. The flume was 750 cm long, 30 cm wide and 50 cm deep, as shown in Fig. 3. The flume was equipped with a pump connected to a water tank that could produce a recirculating current in the flume. In the tank, a refrigeration system could lower down the water temperature to nearly 0 ºC when water passed through the tank. A transducer was used to control the flux. The velocity could be read from an on-line ultrasonic flowmeter (GL/SAZ2-AMF-DN80- 103-0001-000-4.0; Range: 0.3 m/s ~ 12 m/ s). The turbulent wave was made by an electromagnetic shaker fixed at the end of the flume. And the wave height was kept at 30 mm. The virtual depth of the flume was controlled by the height of a weir at the outlet.

Experiment set up

The starting point was set at the position of 100 cm from the inlet. The following part about 500 cm was set as the simulating reach. The virtual height was 30 cm. The tests were conducted at about 5 ºC and the working conditions were shown in Table 1. When the slick's leading edge passed every 50 cm, the time and the position of the tailing edge were recorded, so that the drifting speed and the length of oil slick could be obtained. For the oil spreading under ice, the diesel oil was poured into the water covered by an ice sheet which was 500 cm long, 30 cm wide and 5 cm thick. The roughness of the ice sheet is determined as 0.035 cm by the optical probe method (Li *et al.*, 2007b), far lower than the equilibrium thickness of the oil slick calculated according to Eq. 29.

According to the Eqs. 13, 14 and 21, the slick's dispersion dimension can be obtained by subtracting the spreading dimension from the slick's recorded length. The slick's length at different time can be obtained by means of interpolating on the base of experimental data. The slick's one-dimensional spreading dimension under ice was obtained by measuring the slick's length in the calm water.

RESULTS AND DISCUSSION
Determination of the dispersion coefficient

The values of K_x and β for different spillages at different velocities were presented in Table 1, from which can be seen that K_x decreased a little as the spillage increased because the thicker slick was more difficult to be elongated at the same velocity and the dispersion dimension was smaller. K_x was closely related to the flow velocity as it increased from 3 cm/s to 12 cm/s. However, β fluctuated at about 1.5 and 0.4 on the open water and ice-covered water, respectively. This implied that the dispersion coefficient can still be expressed in the form of βDu^* even in different hydraulic conditions. It was worthwhile to notice that K_x of the under-ice slick was much smaller than that in open water because the ice sheet weakens the turbulent wave and the friction also restricts the slick from elongating to some extent (Zhao *et al.*, 1987). On the other hand, due to the smaller spreading dimension under ice, the slick is thicker and therefore more difficult to be dispersed (Yapa and Chowdhury, 1991). The rangeability of K_x is very small and the mean value may be adopted though K_x is not a constant for different amount of oil.

Fig. 3: The test flume line, commercially available 0 # diesel fuel was chosen. The viscosity is 8.5-9.5 mm/s at 5 ºC, density is 0.835 g/cm, and freezing point is -2C

Sensitivity analysis for the dispersion coefficients

The sensitivity analysis for the dispersion dimension should be considered as K_x changed a little for different amounts of oil. The object function will not be so sensitive to parameters if the sensitivity is small and the model can be called a comparatively stable system (Zhen and Chen, 2003). Assuming the rangeability of K_x is ±10 %, the sensitivity can be obtained according to the following formula (Zhen and Chen, 2003).

$$S^L_{K_x} = (\frac{dL}{dK_x})(\frac{K_x}{L^*})$$ (32)

Where $S^L_{K_x}$ is the sensitivity of the dispersion dimension as K_x being the parameter. L^* is the slick's dispersion dimension after 20 s. K_x is the dispersion coefficients of 3 L oil for the open and ice-covered water. The variable range of the dispersion dimension can be calculated as:

$$\frac{\Delta L}{L^*} = S^L_{K_x}(\frac{\Delta K_x}{K_x})$$ (33)

Where $\Delta K_x/K_x$ is the rangeability of K_x. The sensitivity for the dispersion coefficients and the variable range of the dispersion dimension were shown in Table 2.

Effect of wave on the dispersion coefficient

In addition to the velocity and oil volume, the wave is another factor to affect the slick's dispersion dimension. The slick's dispersion dimensions under different wave heights (WH) were investigated. The relations of β and WH were shown in Fig.4 and 5 for the open water and ice-covered water. The amount of oil was 2 L and the test procedure was the same as above.

In Fig.4, it can be seen that β changed between 0.3 and 3.65 when WH increased to 100 mm. β fluctuated around 1.5 for a wide range of WH, nearly from 20 mm to 70 mm. When WH was less than 20 mm or more than 60 mm, β decreased and increased rapidly. The fitting curves were shown in the local Fig. 4a and b for these two situations and the fitting equations were also given with the correlation coefficients being higher than 0.991. Due to the presence of wave crests and troughs, the conk surface area is larger in comparison with the calm water on which the surface is flat. Assuming the horizontal shearing force is a constant, the slick will be elongated at the position of wave crests and troughs and the elongating amplitude may be bigger as the wave height increases (Li *et al.*, 2007a). However, the continuous slick was hard to be elongated further once WH exceeded a certain value due to the viscous forces and surface-tension (Wang *et al.*, 2005; Li *et al.*, 2007b). This implied that the expressions of K_x were almost the same for the moderate wave disturbance. The distinct increase of β under the high WH was due to the rupture of the continuous oil slick, which was observed in the test.

Fig. 5 showed the relation between β and WH under ice. Due to the ice sheet, WH could not increase further after it exceeded 60 mm in the present condition. It was observed that β increased until WH exceeded 20 mm, and then the increasing rate decreased remarkably and also β stayed at about 0.4 for a wide range of WH. In the experimental condition, the fitting curve was obtained by means of exponential fitting using MATLAB and the fitting equation was also given with the correlation coefficient being 0.986.

Comparing experimental data and numerical calculation

To achieve an impression of how the model performed, it was decided to run some simulations. In short, 3.5 L and 4.5 L of oil were poured onto the open water and ice-covered water at the velocity of 6 cm/s and 12 cm/s, respectively. The WH was kept at 30 mm. However, K_x was obtained from Table 1 by means of interpolating on the base of values.

Table 1: Values of K_x and β for varying spillage at different velocities

Volume of oil (L)	Velocity (cm/s)	K_x (cm^2/s)	β
1	3, 6, 9, 12	5.88, 10.86, 16.67, 22.08	1.633, 1.508, 1.543, 1.533
2	3, 6, 9, 12	5.60, 10.49, 16.15, 22.06	1.555, 1.456, 1.496, 1.532
3	3, 6, 9, 12	5.04, 9.85, 15.91, 21.53	1.399, 1.368, 1.473, 1.495
4	3, 6, 9, 12	4.50, 9.77, 15.29, 20.98	1.250, 1.357, 1.416, 1.457
5	3, 6, 9, 12	4.34, 9.53, 15.20, 20.62	1.205, 1.323, 1.407, 1.432
1*	6, 9, 12	3.01, 4.51, 5.64	0.418, 0.418, 0.392
2*	6, 9, 12	2.84, 4.47, 5.57	0.394, 0.414, 0.387
3*	6, 9, 12	2.80, 4.41, 4.46	0.390, 0.408, 0.379
4*	6, 9, 12	2.74, 4.39, 5.33	0.380, 0.407, 0.370
5*	6, 9, 12	2.69, 4.29, 5.28	0.375, 0.398, 0.366

Table 2: Sensitivity and rangeability of the slick's dispersion coefficients

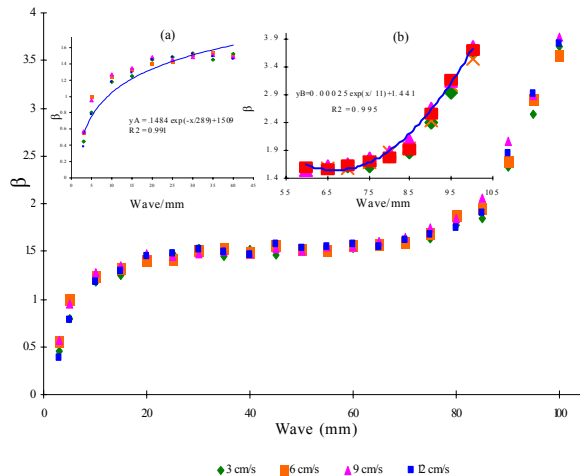| Velocity (cm/s)		3	6	9	12
Open water	S^L_{Kx}	0.47	0.45	0.49	0.47
	$\Delta L/L*$	±4.7%	±4.5 %	±4.9 %	±4.7%
Ice-covered water	S^L_{Kx}	-	0.48	0.49	0.43
	$\Delta L/L*$	-	±4.8 %	±4.9 %	±4.3 %

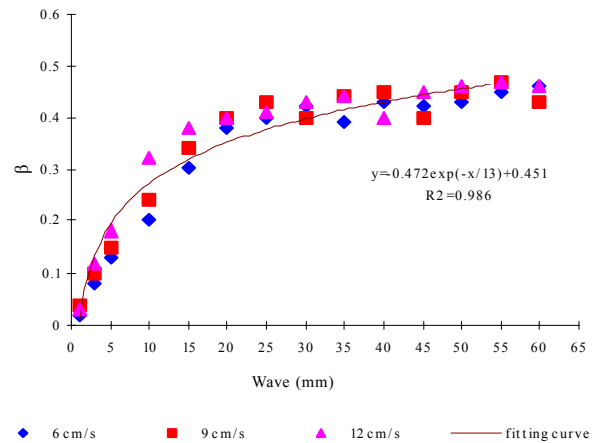Fig. 4: Effect of the wave height on the β in the open water

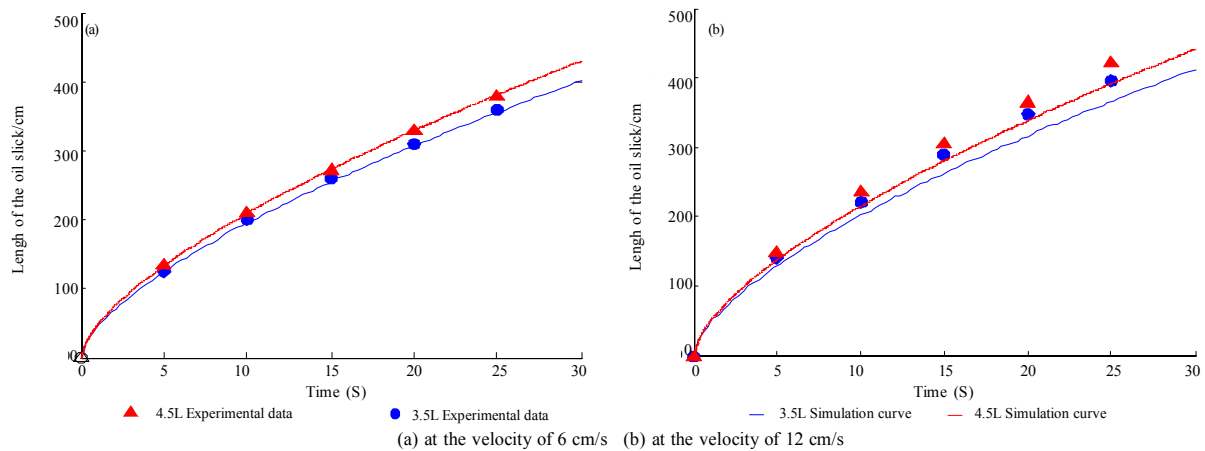Fig. 5: Effect of the wave height on the β under the ice cover

(a) at the velocity of 6 cm/s (b) at the velocity of 12 cm/s
Fig. 6: Comparison of model simulation with experimental data in open water

(a) at the velocity of 6 cm/s   (b) at the velocity of 12 cm/s
Fig. 7: Comparison of model simulation with experimental data under ice
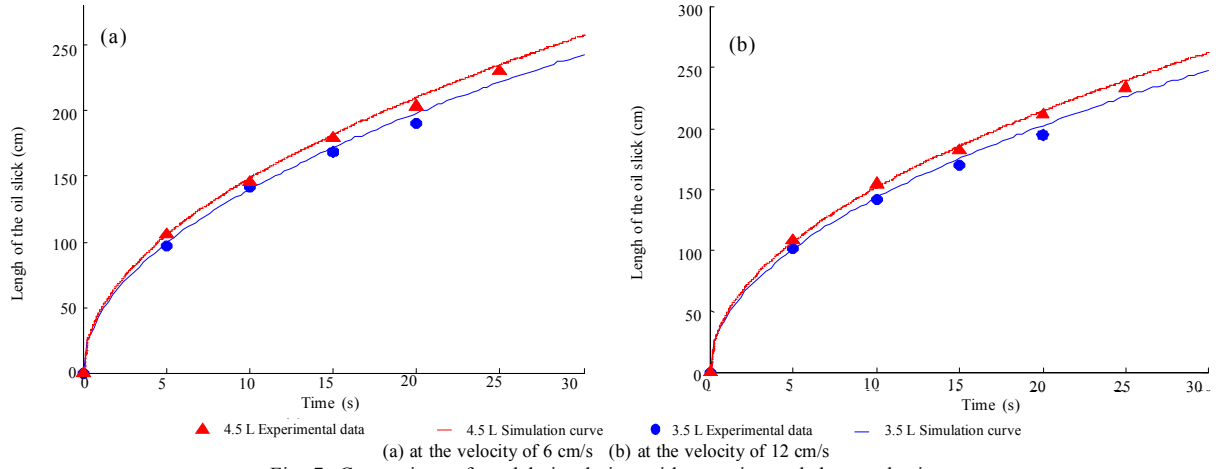
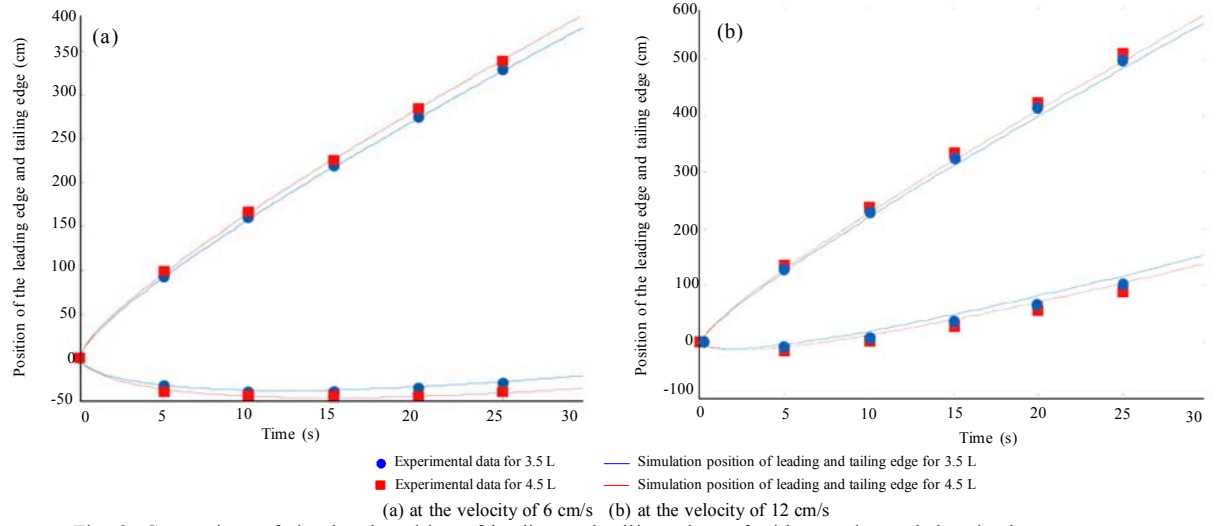(a) at the velocity of 6 cm/s   (b) at the velocity of 12 cm/s
Fig. 8: Comparison of simulated position of leading and tailing edges of with experimental data in the open water

(a) at the velocity of 6 cm/s   (b) at the velocity of 12 cm/s
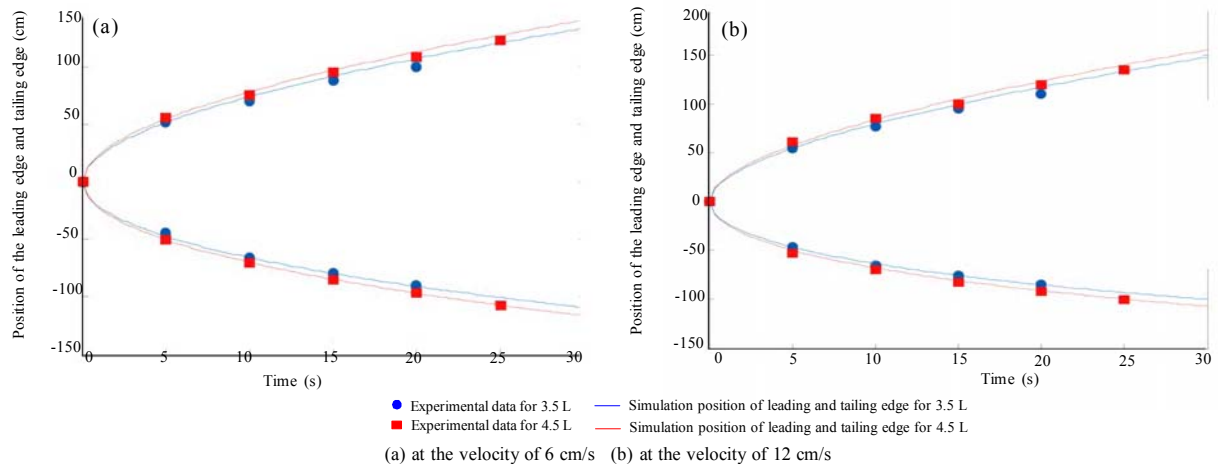Fig. 9: Comparison of simulated position of leading and tailing edges of with experimental data under ice

The length of the oil slick during the gravitation-inertial phase could be calculated according to Eqs. 13, 14 and 21. The duration was calculated according to Eq. 15. In Fig. 6, it was found that the calculated and experimental results matched very well although it underestimated the slick's length a

ttle, because the trailing part of the slick is so thin that it disengages from the main body of the slick due to the disturbance of the water. At the end of the simulation period, the spreading dimensions were 333 cm and 356 cm and the dispersion dimensions were 23 cm and 21 cm for 3.5 L and 4.5 L of oil at 6 cm/s. With the velocity increasing to 12 cm/s, the spreading dimension did not changed very much while the dispersion dimension increased to 32.6 cm and 32.1 cm for 3.5 L and 4.5 L of oil respectively. It confirmed that the dispersion dimension was related to the flow velocity.

Fig. 7 showed the comparison of the simulation and recorded data under ice. It was found that the experimental results were a little smaller than the calculated results. It may be due to the little difference in the roughness of the ice sheets, which resulted in the different frictional resistance between the ice and oil (Yapa and Chowdhury, 1991). Meanwhile, it was observed that there was some oil adhered on the bottom surface of the ice sheet when the slick flowed away. The lost amount of oil might be another reason for the shorter slick's length in the test.

Figs. 8 and 9 demonstrated the comparison of the positions of leading and tailing edges available from the experiments with the results obtained from Eqs.26 and 27. It was found that the relative errors between the calculated and recorded results were less than 5 % both for the open water and ice-covered water. As the velocity increased, the slick would drift faster and contaminate area would be larger. Furthermore, the under-ice slick would travel much slower and the slick's length would be shorter. Comparing Fig. 8a and Fig. 9a, 3.5 L of oil, at 6 cm/s, after 20 s, the under-ice slick travelled only 100 cm whereas the slick travelled 275 cm in the open water. The slick's lengths were approximately 190 cm and 310 cm, respectively. It was good news to clean the oil under ice due to the smaller contaminative area.

CONCLUSION

The velocity profile across the vertical section of the oil slick on moving water was found to be the combination of linear and parabolic distribution, on the base of which a model including the oil spreading and dispersion was developed to simulate the early movement of an oil spill

in the flow field. The dispersion coefficient (K_x) was determined via the flume test. The results indicated that K_x could be expressed in the form of βDu^* and changed from 4.34 cm^2/s to 20.08 cm^2/s in the open water and from 2.69 cm^2/s to 5.64 cm^2/s in the ice-covered water as the velocity increased. However, β was found to be a constant in different hydraulic conditions. In the open water, β fluctuated around 1.5 when WH changed from 20 mm to 70 mm. Under ice, β increased until WH increased to 20 mm and maintained at about 0.4. The comparisons of the simulated results with experimental data are satisfactory over the simulated period. However, further verification is needed before a conclusion is made on the quality of the model for its application to a real oil spill.

REFERENCES

Abbaspour, M.; Shojaee, M. N., (2009). Innovative approach to design a new national low speed wind tunnel. Int. J. Environ. Sci. Tech., 6 (1), 23-34 (**12 pages**).

Alihosseini, A.; Taghikhani, V.; Safekordi, A. A.; Bastani, D.; (2010). Equilibrium sorption of crude oil by expanded perlite using different adsorption isotherms at 298.15 k. Int. J. Environ. Sci. Tech., 7 (3), 591-598 (**8 pages**).

Boufadel, M. C.; Du, K.; Kaku, V.; Weaver, J., (2007). Lagrangian simulation of oil droplets transport due to regular waves. Environ. Model. Software, 22 (7), 978-986 (**9 pages**).

Brovchenko, I.; Kuschan, A.; Maderich, V.; Zheleznyak, M., (2002) The modelling system for simulation of the oil spills in the Black Sea. 3rd EuroGOOS Conference: Building the European capacity in operational oceanography., 192.

Elliott, A. J.; (2004). A probabilistic description of the wind over Liverpool Bay with application to oil spill simulations. Estuar. costal shelf Sci., 61 (4), 569-581 (**13 pages**).

Faksness, L. G.; Brandvik, P. J., (2008). Distribution of water soluble component from oil encapsulated in sea ice, Summary of results from three different field seasons. Cold Reg. Sci. Tech., 54 (2), 106-114 (**9 pages**).

Fingas, M. F.; Hollebone, B. P., (2003). Review of behaviour of oil in freezing environments. Mar. Pollut. Bull., 47 (9-12), 333-340 (**8 pages**).

GjØsteen, J. K. Ø., (2004). A model for oil spreading in cold waters. Cold Reg. Sci. Tech., 38 (2-3), 117-125 (**9 pages**).

Gong, R.; Liang, J.; Chen, J.; Huang, F., (2009). Removal of bisphenol A from aqueous solution by hydrophobic sorption of hemimicelles. Int. J. Environ. Sci. Tech., 6 (4), 539-544 (**6 pages**).

Guo, Y. H., (2008). Teaching materials of boundary theory. University of science and technology of China press, 29-55 (**7 pages**).

Guo, Y. W.; Liu, D.; Zhong, B. C.; Wang, D. Z., (2008). Experimental investigations of wind effect on the oil spill spread and drift. Chinese J. Hydrodynamics, 23 (4), 446-452 (**7 pages**).

Guo, W. J.; Wang, Y. X., (2009). A numerical oil spill model based on a hybrid method. Mar. Pollut. Bull., 58 (5), 726-734 (**9 pages**).

Hibbs, D. E.; Gulliver, J. S.; Voller, V. R.; Chen, Y. F., (1999). An aqueous concentration model for riverine spills. J. Hazard. Mater., 64 (1), 37-53 (**17 pages**).

Husseien, M.; Amer, A. A.; El-Maghraby, A.; Taha, N. A., (2009). Availability of barley straw application on oil spill clean up. Int. J. Environ. Sci. Tech., 6 (1), 123-130 (**8 pages**).

Izumiyama, K.; Konno, A., (2002). Experimental study on the spreading of oil under ice covers. In: Proc. of The Twelfth (2002) Int. Offshore and Polar Engineer. 26-31 May. Kitakyushu, Japan.

Li, F. L.; Tan, G. Y.; Duan, H. F.; Hao, J. G., (2007a). New development in research of non-contact surface roughness measurement, Laser and anfrared, 37 (6), 498-502 (**5 pages**).

Li, Z. J.; Hollebone, B.; Fingas, M.; Fieldhouse, B., (2007b). Physical model technique on the behaviors of oil spills in grease ice under wave actions. J. Dalian Maritime University, 33 (4), 91-95 (**5 pages**).

Liu, H. Z.; Shu, H. J., (1991). Theory of boundary. China Communications Press, 66-78 (**13 pages**).

Liu, W. F.; Sun, Y. G., (2009). Study and improvement of oil spill simulation methods. J. East China Normal University (Natural Science), 3, 90-97 (**8 pages**).

Nagheeby, M.; Kolahdoozan, M., (2010). Numerical modeling of two-phase fluid flow and oil slick transport in estuarine water. Int. J. Environ. Sci. Tech., 7 (4), 771-784 (**14 pages**).

Qi, P. S.; Shao, Z. G.; Li, Y. Z., (2010). The mathematical modeling and simulation on abnormal evaporation of spilled oil at low temperature. J. Harbin Institute of Tech., 42 (6), 893-898 (**6 pages**).

Rajakumar, R.; Meenambal, T.; Rajesh Banu, J.; Yeom, I. T., (2011). Treatment of poultry slaughterhouse wastewater in upflow anaerobic filter under low upflow velocity. Int. J. Environ. Sci. Tech., 8 (1), 149-158 (**10 pages**).

Reed, M.; Johansen, Ø.; Brandvik, P. J.; Daling, P.; Lweis, A.; Ficco, R.; Mackay, D.; Prentki, R., (1999). Oil spill modeling towards the 20th century: Overview of the state of the art. Spill Sci. Tech. Bull., 5 (1), 3-16 (**14 pages**).

Sayre, W. W.; Chang, F. M., (1969). A laboratory investigation of open channel dispersion processes for dissolved, suspended, and floating dispersants. United States Geological Survey, 11 (51), E1-E71 (**8 pages**).

Shen, H. T.; Yapa, P. D., (1988). Oil Slick Transport in Rivers. J. Hyd. Eng., 114 (5), 529-543 (**15 pages**).

Tuzkaya, G.; Ozgen, A.; Ozgen, D.; Tuzkaya, U. R., (2009). Environmental performance evaluation of suppliers: A hybrid fuzzy multi-criteria decision approach. Int. J. Environ. Sci. Tech., 6 (3), 477-490 (**14 pages**).

Wang, P.; Li, Z. J., (2003). A Primary Numerical Model of Oil Spilling in Icing Sea. J. Glaciology Geocryology, 25 (2), 334-337 (**4 pages**).

Wang, S. D.; Shen, Y. M.; Zheng, Y. H., (2005). Two-dimensional numerical simulation for transport and fate of oil spill in seas. Ocean Eng., 32 (13), 1556-1571 (**16 pages**).

Wu, J.; He, Ch., (2010). Experimental and modeling investigation of sewage solids sedimentation based on particle size distribution and fractal dimension. Int. J. Environ. Sci. Tech., 7 (1), 37-46 (**10 pages**).

Yapa, D.; Chowdhury, T., (1991). Spreading of oil spilled under ice. J. Hyd. Eng., 116 (12), 1468-1483(**16 pages**).

Yapa, D.; Shen, H.; T., (1994). Modeling river oil spill: A review. J. Hyd. Res., 32 (5), 765-782 (**18 pages**).

Yu, J. A.; Zhang, B.; Liu, Q. Z.; Chen, W. B.; Wang, R. S., (1999). Numerical experiment on the behavior of oil spills in ice-infested waters in the bohai sea. Oceanoiogia et limnologia sinica, 30 (5), 552-557 (**6 pages**).

Zhang, Z. X.; Dong, Z. N., (1998). Viscous fluid mechanics. Tsinghua University Press, 52-101 (**50 pages**).

Zhao, W. Q.; Wu, Z. H.; Zhou, K. Z., (1987). Spreading, drifting and dispersion of the crude oil at sea—the review of the study on oil contamination at sea. J. Chendu University Sci. Tech., 33 (1), 141-149 (**9 pages**).

Zhen, T.; Chen, C. Y., (2003). Environmental systems and mathematical model. Chemical Industrial Press, 29-30 (**2 pages**).

AUTHOR (S) BIOSKETCHES

Peishi, Q., Ph.D., Professor in the State Key Laboratory of Urban Water Resources and Environment, Harbin Institute of Technology, Harbin, 150090, China. E-mail: *qipeishi@163.com*

Zhiguo, S., Ph.D., Research student in the State Key Laboratory of Urban Water Resources and Environment, Harbin Institute of Technology, Harbin, 150090, China. E-mail: *shaozhiguo003@163.com*

Yunzhi, L., Lecturer in the State Key Laboratory of Urban Water Resources and Environment, Harbin Institute of Technology, Harbin, 150090, China. E-mail: *linyunzhi0907@163.com*